

# Radical Loss in a Chain Reaction of CO and NO in the Presence of Water: Implications for the Radical Amplifier and Atmospheric Chemistry

C. M. MIHELE, M. MOZURKEWICH, D. R. HASTIE

Centre for Atmospheric Chemistry and Department of Chemistry, York University, 4700 Keele St., Toronto, Ontario M3J 1P3

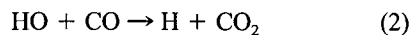
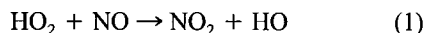
**ABSTRACT:** Atmospheric pressure rate coefficients for the loss of HO<sub>2</sub>, CH<sub>3</sub>O<sub>2</sub>, and C<sub>2</sub>H<sub>5</sub>O<sub>2</sub> radicals to the wall of a  $\frac{1}{4}$ " Teflon tube have been measured. In dry air, they are  $2.8 \pm 0.2 \text{ s}^{-1}$  for HO<sub>2</sub> and  $0.8 \pm 0.1 \text{ s}^{-1}$  for both CH<sub>3</sub>O<sub>2</sub> and C<sub>2</sub>H<sub>5</sub>O<sub>2</sub> radicals. The rate coefficient for HO<sub>2</sub> loss increases markedly with the relative humidity of the air; however, the organic radicals show no such dependence. These data are used in a kinetic model of the radical amplifier chemistry to investigate the reported sensitivity to water concentration. The increased wall loss accounts for only some of the observed water dependence, suggesting there is an unreported water contribution to the gas phase chemistry. Including the reaction of the HO<sub>2</sub>/water adduct with NO to yield HNO<sub>3</sub> or HOONO into the mechanism is shown to provide a better simulation of the observed water dependence of the radical detector. This reaction would also be important in atmospheric chemistry as it provides an additional loss mechanism for both radicals and NO<sub>x</sub>. © 1999 John Wiley & Sons, Inc. *Int J Chem Kinet* 31: 145–152, 1999

## INTRODUCTION

The radical amplifier is a kinetics-based instrument used for the measurement of the total concentration of radicals in a gas phase sample [1,2]. It has found use in a number of atmospheric chemistry field studies [3–

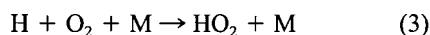
7] and, because of this widespread use, a number of such instruments have recently been compared against each other and an independent method [8].

The principle behind the technique is that a chain reaction can be set up by doping the sample with NO and CO. Odd hydrogen radicals (HO<sub>x</sub> = HO and HO<sub>2</sub>) enter into a chain reaction

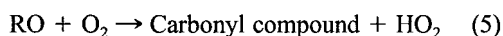
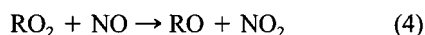


---

Correspondence to: D. R. Hastie  
Contract grant Sponsor: Atmospheric Environment Service of Environment Canada



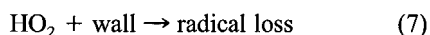
Furthermore, organic radicals ( $\text{RO}_x = \text{RO} + \text{RO}_2$ , where R is an organic group) are largely converted to  $\text{HO}_x$  radicals through the reactions



Thus,  $\text{RO}_x$  radicals, after this conversion, can cycle through reactions (1)–(3). Chain termination occurs when radicals are lost, either through gas phase termination reactions such as



or to the walls of the reactor such as



This basic chemistry represents a simple straight chain mechanism characterised by the chain length (CL), the number of times the radical passes through the cycle before being lost. The value of this system as a radical detector comes from the fact that one  $\text{NO}_2$  molecule is produced for each time through the cycle, thus converting the small number of radicals into a larger number of  $\text{NO}_2$  molecules that can be measured. The radical concentration is then inferred from a measurement of the  $\text{NO}_2$  produced by the chain,  $\delta[\text{NO}_2]$ , and the chain length.

$$[\text{RO}_x] = \delta[\text{NO}_2]/\text{CL} \quad (I)$$

The chain length is determined by the addition of a known concentration of radicals at the inlet of the instrument [9]. Other  $\text{NO}_2$  sources that could be interferences are negated by regularly removing CO from the reactor. In the absence of CO the chain reaction cannot occur and the interferences can be determined [2].

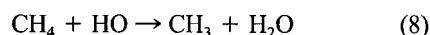
A full description of the chemistry of the radical amplifier consists of a mechanism of some 40 reactions which cover the dominant reactions over a wide range of experimental conditions and atmospheric species [2]. Models of this system have been successful in explaining the chemistry and the performance of the technique.

Recent experimental work on the radical amplifier has shown that the chain length decreases with increasing water vapor concentration in the reactor [10]. At

40% relative humidity, a 50% decrease in chain length, compared to dry air, is reported. Current models are unable to explain this observation. The decrease in chain length could be due to a decrease in the rate of the chain propagation reactions or an increase in the rate of termination reactions. The dominant termination reaction in most radical amplifiers is radical loss to the walls of the reactor. In this paper we present a study where the rate of radical loss to the walls of the reactor is measured as a function of water vapor concentration. These data are then used in a kinetic model of the radical amplifier chemistry to try to rationalize the reported behavior and to look for any additional water dependence.

## EXPERIMENTAL

The experimental system is shown in Figure 1. Mixing ratios of 10 to 150 pptv of  $\text{HO}_2$  radicals were generated from the photolysis of water in air at atmospheric pressure and quantified using the ozone produced as an actinometer [9]. The photolysis yields H atoms, which react rapidly with oxygen to give  $\text{HO}_2$  and an equal number of HO radicals. For  $\text{HO}_2$  experiments, 100–200 ppmv of CO was added to the air stream to convert the HO to  $\text{HO}_2$  through reactions (2) and (3). For experiments where organic radicals were required, the CO was replaced with the appropriate alkane. For example, methyl peroxy radicals were formed from the HO radicals and methane via



During the course of this work it was found that the rate of wall loss for the  $\text{HO}_2$  radicals was at least double that for the organic radicals. This provided a method to produce a cleaner source of organic radicals ( $\text{RO}_2$ ). The  $\text{HO}_2$  radical concentration was found to drop below the detection limit after passing through 2 m of Teflon tubing. Thus, for the organic peroxy radical studies the mixture of  $\text{HO}_2$  and  $\text{RO}_2$  radicals produced by the source were passed down this tubing and the radicals remaining, although at reduced concentration, were assumed to be organic peroxy radicals.

This source produced radicals in essentially dry air, therefore an additional flow of wet zero air was required to produce air of the desired humidity for the experiments. A flow of up to  $1.04 \text{ l min}^{-1}$  of air was saturated with water vapor, in a temperature stabilized bubbler, and sampled together with the dry air containing the radicals. Varying the flow of the saturated air produced from 0 to 70% relative humidity at  $21^\circ\text{C}$

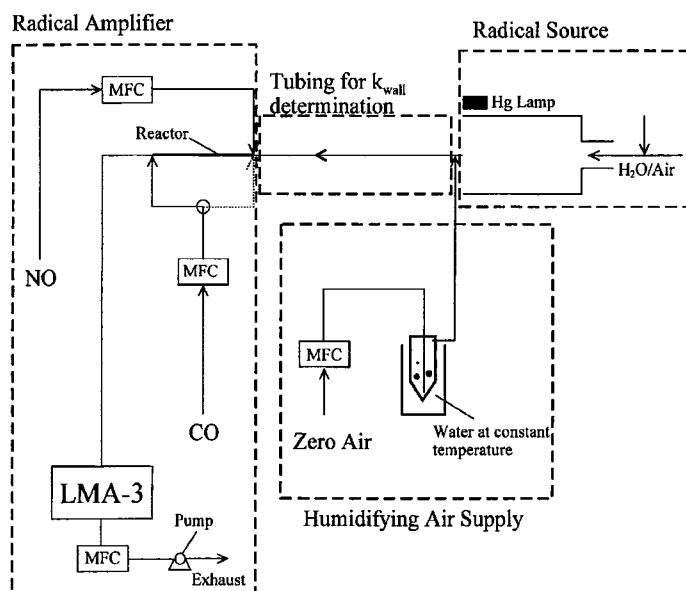


**Figure 1** Experimental apparatus used in this study. MFC; mass flow controller; LMA-3;  $\text{NO}_2$  detector.

in the tubing under test (Figure 1). Calculated water vapor concentrations, based on the saturated water vapor pressure and the air flows, agreed with dew points measured using an EG&G Model 911 dew point hygrometer.

Radical concentrations were measured using a radical amplifier as described in Arias and Hastie [4] as shown on the left side of Figure 1. Air entering the reactor, a 1.5 m section of  $\frac{1}{4}$ " OD PFA Teflon tubing, was mixed with NO and CO to give mixing ratios of 2 ppmv and 4%, respectively. The flow of  $1.6 \text{ l min}^{-1}$  gave a residence time of 1.0 s, much longer than required for the chain reaction to be completed. All flows were regulated by mass flow controllers (MFC) and the Luminol based  $\text{NO}_2$  detector (Scintrex LMA-3) was operated in the linear regime by addition of approximately 10 ppbv of  $\text{NO}_2$  from a thermostated permeation device. All experiments were performed with radical concentrations where the  $\text{NO}_2$  production is linear [2].

To ensure that the parameters determined in this experiment could be used in the analysis of the radical detector, the wall loss rate coefficient was determined for the same  $\frac{1}{4}$ " OD PFA Teflon tubing as used for the reactor. Reaction time was varied by changing the length of tubing and was determined from the length and the air flow, assuming plug flow. This allowed the radical loss to be measured for up to 0.4 seconds. Since varying the water concentration involved changes to

the air flows at the entrance to the tubing, a series of dry air tests were made to ensure that the concentration of radicals could be predicted from the dilution of the radical source by the additional air flow. At the radical concentrations and times used, the gas phase self reaction of  $\text{HO}_2$  does not need to be considered, as it consumes less than 2% of the  $\text{HO}_2$ .

A typical wet or dry experiment was performed by measuring the  $\text{NO}_2$  produced by the radical amplifier for a minimum length of tubing,  $\delta[\text{NO}_2]_0$ , and for a range of other lengths,  $\delta[\text{NO}_2]$ . Since the kinetics is first order (see later), the ratio of the  $\text{NO}_2$  concentrations produced represents the ratio of the radical concentrations and is independent of the absolute concentration of the radicals and the sensitivity of the  $\text{NO}_2$  detector. Thus there was no need to apply a correction for the variation in radical amplifier sensitivity with water vapor concentration [10].

The impact of water on the chain length of the radical amplifier was also determined, for comparison with the model. In this case the tubing section was removed so the water was added directly into the reactor of the radical amplifier. The ratio of the  $\text{NO}_2$  produced in the absence and presence of water for exactly the same air flows is the ratio of the chain lengths and is independent of the absolute concentration of the radicals and the sensitivity of the  $\text{NO}_2$  detector, provided the experiments were performed in the linear region of the detector.

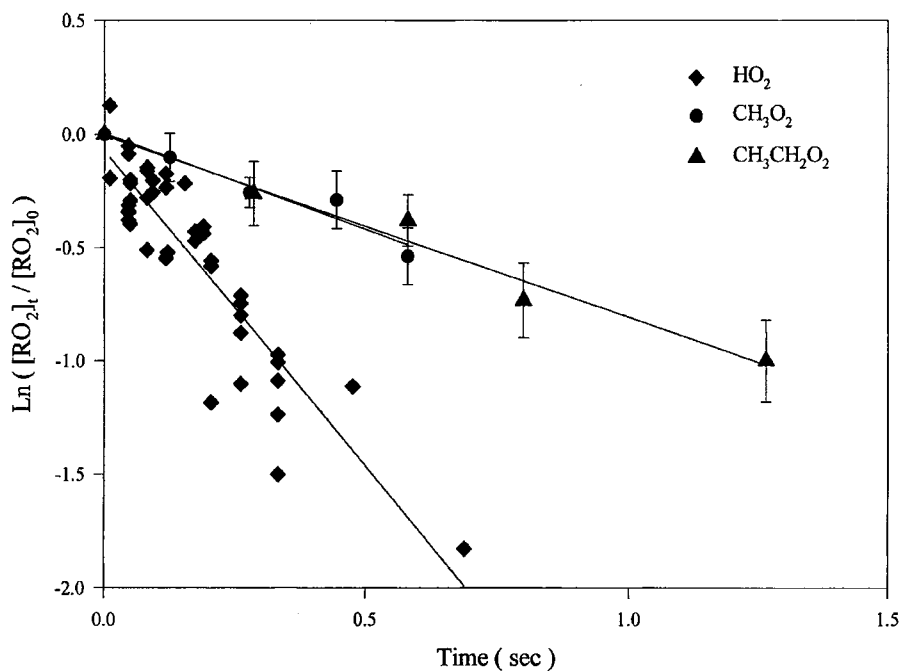


Figure 2 First order kinetic plot for the loss of radicals to the wall of the Teflon tube.

## RESULTS

### Rate Coefficient for Radical Loss

The loss of radicals in the Teflon tube was found to have a significantly better fit to first order than to second order kinetics. The data for radical loss in dry air is shown in Figure 2, where  $\ln(\delta[\text{NO}_2]/\delta[\text{NO}_2]_0)$  is plotted against time for three radicals:  $\text{HO}_2$ ;  $\text{CH}_3\text{O}_2$ ; and  $\text{C}_2\text{H}_5\text{O}_2$ . These data represent all data points obtained from six experiments for  $\text{HO}_2$  radicals, and three experiments each for  $\text{CH}_3\text{O}_2$  and  $\text{C}_2\text{H}_5\text{O}_2$  radicals. The rate coefficient  $k_{\text{wall}}$  obtained from the slope of the  $\text{HO}_2$  loss is  $2.8 \pm 0.2 \text{ s}^{-1}$ , and for both  $\text{CH}_3\text{O}_2$  and  $\text{C}_2\text{H}_5\text{O}_2$  it is  $0.8 \pm 0.1 \text{ s}^{-1}$ . The value for the  $\text{HO}_2$  radical loss is consistent with the value of  $2.5 \text{ s}^{-1}$  that has been found to be necessary to successfully model the chain lengths obtained in at least two detectors [2,11]. The factor of three difference in wall loss rates probably reflects the lower polarity of the  $\text{RO}_2$  radicals.

We can calculate an upper limit for  $k_{\text{wall}}$  in this system using the Gormley-Kennedy (G-K) equation [12]. This equation calculates the rate of diffusive transport of radicals to the walls of the reactor. Once a radical diffuses to the wall, it will undergo many collisions with the wall in the time before diffusion carries it away again. As a result, a wall loss rate will not deviate significantly from that calculated from the

G-K equation unless the reaction probability is much less than unity. For the apparatus and conditions used in these experiments, the G-K equation gives a  $k_{\text{wall}}$  of  $20 \text{ s}^{-1}$ , much higher than any of the measured values. This shows that the rate of radical loss is not governed by diffusive transport to the walls, but rather by the low reaction probability  $\gamma$ , for reactions on the walls of the tubing. Under these conditions,  $\gamma$  can be determined from  $k_{\text{wall}}$  using [12]

$$\gamma = \frac{2Rk_{\text{wall}}}{\bar{c}} \quad (\text{II})$$

where  $R$  is the tube radius (0.24 cm) and  $\bar{c}$  is the average speed of the gas molecules. This yields reaction probabilities of  $3.1 \times 10^{-5}$ ,  $1.1 \times 10^{-5}$ , and  $1.2 \times 10^{-5}$  for  $\text{HO}_2$ ,  $\text{CH}_3\text{O}_2$ , and  $\text{C}_2\text{H}_5\text{O}_2$  radicals respectively. Previously determined wall loss rates have yielded values of  $\gamma = 3 \times 10^{-4}$  for  $\text{HO}_2$  on glass [13,14]. The smaller value on Teflon is likely related to the lower polarity of this surface.

The variation in  $k_{\text{wall}}$  with relative humidity for the three radicals is shown in Figure 3. For the  $\text{HO}_2$  radical, the rate coefficient increases by more than a factor of two for an increase in relative humidity from zero to 50%. In contrast, the organic radicals show almost no sensitivity to the presence of water vapor, at least up to 70% relative humidity. This water de-

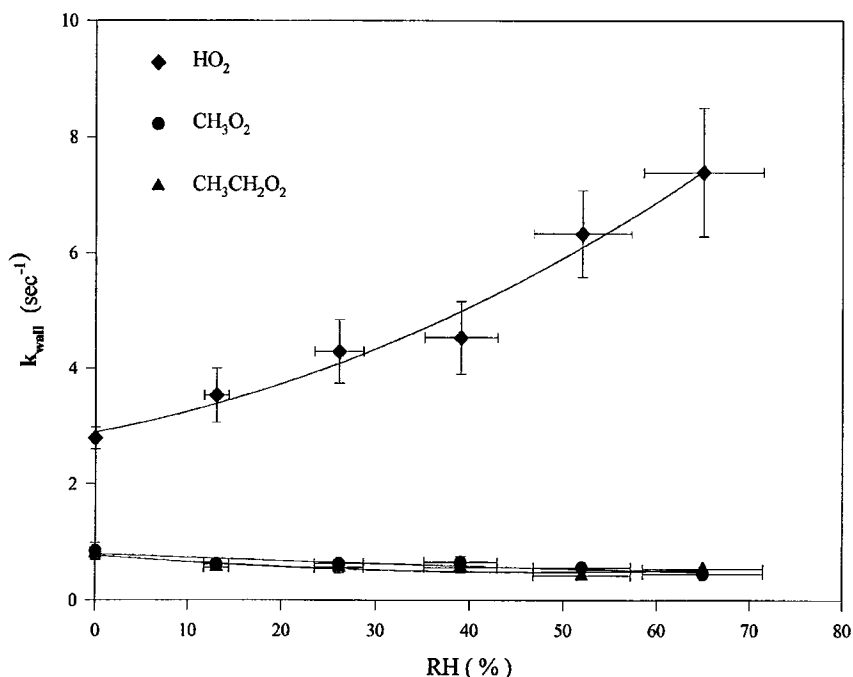


**Figure 3** Variation of the rate coefficient for loss of radicals to the wall of the Teflon tube as a function of relative humidity.

pendence for  $\text{HO}_2$  but not  $\text{RO}_2$  is consistent with the known interaction of  $\text{HO}_2$  radicals with water and the lack of a reported interaction with  $\text{RO}_2$ . It should be noted that, even at the highest water concentrations,  $k_{\text{wall}}$  is still a factor of three below that given by the Gormley-Kennedy equation.

### Modeling of the Radical Amplifier Kinetics

The purpose of this work is to develop a better model of the performance of the radical amplifier and to identify the cause of the dependence on water vapor. This was tested by comparing model predictions of the chain lengths for  $\text{HO}_2$  against those determined by experiment.

The chemistry of the radical amplifier was simulated by a model of 28 gas phase reactions and 2 surface reactions as detailed in Table I. This mechanism is basically that used previously [2,11,15], except that: only the inorganic reactions are considered; the measured wall loss rate coefficients are used; and the water dependence of the third order reactions of HO with NO [16],  $\text{HO}_2$  with  $\text{HO}_2$  [17], and  $\text{HO}_2$  with  $\text{NO}_2$  [18] have been included. Results are reported in terms of the ratios of the chain lengths for wet and dry air. This model produced satisfactory simulations with dry

air. The results of these simulations are shown with the experimental results in the lower panel of Figure 4. While the simulation shows a decrease in the chain length as the relative humidity increases, the decrease is somewhat underestimated by the model. This implies that the water impact is not only due to the increased wall loss rate. To test for a possible gas phase component to the decrease, a series of experiments were performed where the importance of the wall loss was lessened by operating at higher NO concentrations. Under these conditions the gas phase termination reaction (6) would be more important than the loss of radicals to the reactor wall (7). The results for these experiments, and the modelling of them, are shown in the upper panel of Figure 4. Experimentally, the added water vapor has less effect at higher NO concentrations as would be expected, as the highly sensitive wall loss has less impact. However, the ability of the model to simulate the observations is much worse. It can only account for half of the 40% decrease in chain length induced by the water.

The model includes the known water dependencies in the kinetic data for radical and  $\text{NO}_x$  reactions. Therefore the discrepancy must be due to a water dependence that is not known. The chain length could be decreased by either a decrease in the rate of the gas phase chain propagation reactions, or an increase in the rate of the gas phase termination reactions. The

**Table I** Reactions Used in the Modeling of the Response of the Radical Amplifier to HO<sub>2</sub> Radicals in the Presence of Water

Reaction	Source of Rate Coefficient
<b>Simple Chain Mechanism</b>	
HO <sub>2</sub> + NO → HO + NO <sub>2</sub>	25
HO + CO → H + CO <sub>2</sub>	25
H + O <sub>2</sub> + M → HO <sub>2</sub> + M	25
HO + NO + M → HONO + M	25
HO + NO + H <sub>2</sub> O → HONO + H <sub>2</sub> O	16
<b>HO Radical Reactions</b>	
HO + O <sub>3</sub> → HO <sub>2</sub> + O <sub>2</sub>	25
HO + HNO <sub>3</sub> → H <sub>2</sub> O + NO <sub>3</sub>	25
HO + HONO → H <sub>2</sub> O + NO <sub>2</sub>	25
HO + HNO <sub>4</sub> → H <sub>2</sub> O + NO <sub>2</sub> + O <sub>2</sub>	25
HO + NO <sub>2</sub> + M → HNO <sub>3</sub> + M	25
HO + NO <sub>3</sub> → HO <sub>2</sub> + NO <sub>2</sub>	25
HO + HO → H <sub>2</sub> O + O	25
HO + HO + M → H <sub>2</sub> O <sub>2</sub> + M	25
HO + HO <sub>2</sub> → H <sub>2</sub> O + O <sub>2</sub>	25
HO + H <sub>2</sub> O <sub>2</sub> → H <sub>2</sub> O + HO <sub>2</sub>	25
<b>HO<sub>2</sub> Radical Reactions</b>	
HO <sub>2</sub> + NO <sub>2</sub> + M → HNO <sub>4</sub> + M	25
HNO <sub>4</sub> + M → HO <sub>2</sub> + NO <sub>2</sub> + M	25
HO <sub>2</sub> + O <sub>3</sub> → HO + O <sub>2</sub> + O <sub>2</sub>	25
<b>O<sub>3</sub> Reactions</b>	
NO + O <sub>3</sub> → NO <sub>2</sub> + O <sub>2</sub>	25
NO <sub>2</sub> + O <sub>3</sub> → NO <sub>3</sub> + O <sub>2</sub>	25
NO <sub>3</sub> + NO <sub>2</sub> + M → N <sub>2</sub> O <sub>5</sub> + M	25
N <sub>2</sub> O <sub>5</sub> + M → NO <sub>3</sub> + NO <sub>2</sub> + M	25
<b>Radical Loss at Walls of Vessel</b>	
HO →	Variable
HO <sub>2</sub> →	This work
<b>Water Dependence of HO<sub>2</sub> Reactions</b>	
HO <sub>2</sub> + HO <sub>2</sub> (+H <sub>2</sub> O) → H <sub>2</sub> O <sub>2</sub> + O <sub>2</sub> (+H <sub>2</sub> O)	25
HO <sub>2</sub> + H <sub>2</sub> O → HO <sub>2</sub> H <sub>2</sub> O	18
HO <sub>2</sub> H <sub>2</sub> O → HO <sub>2</sub> + H <sub>2</sub> O	18
HO <sub>2</sub> H <sub>2</sub> O + NO <sub>2</sub> → HO <sub>2</sub> + NO <sub>2</sub> + H <sub>2</sub> O	18
HO <sub>2</sub> H <sub>2</sub> O + NO → HNO <sub>3</sub> H <sub>2</sub> O + H <sub>2</sub> O	proposed

experiments are not able to directly distinguish between these alternatives.

The HO<sub>2</sub> radical and water are known to form an adduct in the gas phase and the equilibrium constant for the adduct formation has been determined [18,19]. The adduct plays a part in the gas phase HO<sub>2</sub> chemistry, producing a strong water dependence in the HO<sub>2</sub> self reaction to produce hydrogen peroxide [17] and

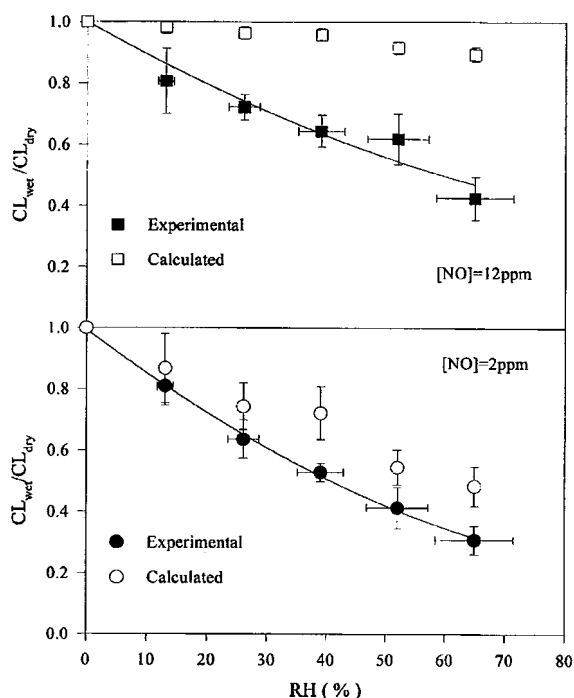
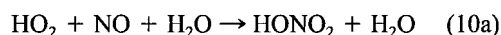


**Figure 4** The observed chain length (CL) of the radical amplifier in the presence of wet air compared to that under dry conditions (solid symbols) compared with that calculated from the kinetic model (open symbols) as a function of relative humidity. Upper and lower panels for NO mixing ratios of 12 ppmv and 2 ppmv in the reactor.

the reaction with NO<sub>2</sub> to produce peroxyxynitric acid [18]. There has been no report of the reaction of the adduct with NO, but since HO<sub>2</sub> is the dominant radical in the radical amplifier, any modification to the kinetics or products of its reactions in the presence of water would impact the chain length.

The adduct could possibly lower the rate coefficient for (1), the HO<sub>2</sub> radical oxidation of NO to NO<sub>2</sub>. However, the presence of a water molecule at the radical center is unlikely to significantly block the reaction site, nor is there evidence for this effect in any kinetic studies. Further, the published equilibrium constants indicate some 7.5% of the HO<sub>2</sub> radicals are present as the adduct, at 40% relative humidity. Even if the adduct was unreactive towards NO, this would only lower the chain length by a maximum of 7.5%, which is much smaller than the observed 40% decrease. The actual effect would be lower still as the propagation rate is not solely governed by reaction (1).

The lack of a viable impact on the bimolecular, chain propagation channel suggests the water impact may be through a termolecular, chain termination channel. In particular, either reaction



or



would have a large impact on the amplifier chemistry by replacing the chain propagating reaction (1) with a chain termination reaction.

In order for the model to simulate the observations, we must include either reaction 10a or 10b with a rate coefficient,  $2.1 \times 10^{-31} \text{ cm}^6 \text{ molec}^{-2} \text{ s}^{-1}$ . This implies a rate coefficient of about  $7 \times 10^{-13} \text{ cm}^3 \text{ molec}^{-1} \text{ s}^{-1}$  for the second order reaction of the adduct with NO if the equilibrium constant for the adduct formation is  $3 \times 10^{-19} \text{ cm}^3 \text{ molec}^{-1}$  [18].

At 40% relative humidity ( $[\text{H}_2\text{O}] = 2.5 \times 10^{17} \text{ molec cm}^{-3}$ ), this would mean that the rate of reaction (10) is just 1% of the rate of reaction (1). Thus, it is not surprising that no water vapor effect has been observed in direct kinetics studies of reaction (1)[20].

### Possible Atmospheric Implications

Whether reaction (10) has any impact on atmospheric chemistry depends on which product is formed and, if the product is peroxyxynitrous acid, its fate. Although reaction (10) is insignificant in comparison with reaction (1) its possible impact on atmospheric chemistry will come from comparison with reaction (11), since this is usually the major sink for both  $\text{HO}_x$  and  $\text{NO}_x$ .



Using the estimated rate coefficient for reaction (10) of  $2.1 \times 10^{-31} \text{ cm}^6 \text{ molec}^{-2} \text{ s}^{-1}$  from above, the atmospheric pressure rate coefficients for reactions (11) and (1) of  $1.4 \times 10^{-11}$  and  $8.3 \times 10^{-12} \text{ cm}^3 \text{ molec}^{-1} \text{ s}^{-1}$  respectively, and box model estimates of  $[\text{HO}]/[\text{HO}_2]$  as 0.01 and  $[\text{NO}_2]/[\text{NO}]$  as 3, the rate of reaction (11) is about 5% that of reaction (1) and only about 8 times faster than reaction (10) at 40% relative humidity. Thus, if the product of reaction (10) is  $\text{HNO}_3$ , this will be a significant, but minor, sink for  $\text{HO}_x$  and  $\text{NO}_x$ .

If the product of reaction (10) is HOONO, it will likely dissociate to form OH and  $\text{NO}_2$ . However, it may also undergo an isomerization to  $\text{HNO}_3$  in the atmospheric aerosol. This isomerization is known to occur efficiently in acidic solutions [21]; therefore, the impact of (10b) will depend on which of the two processes, gas phase dissociation or heterogeneous isom-

erization, is faster. We can use existing data to estimate the rates of both processes.

Koppenol et al. have examined the thermodynamics of HOONO [21]. By assuming that HOONO has the same free energy of solution as  $\text{H}_2\text{O}_2$ , they constructed a thermochemical cycle that yielded a gas phase bond dissociation enthalpy of  $88 \pm 9 \text{ kJ mol}^{-1}$ . However, their assumed free energy of solution ( $33 \text{ kJ mol}^{-1}$ ) implies a Henry's Law constant of  $5.3 \times 10^5 \text{ M atm}^{-1}$ ; this is too large even for  $\text{H}_2\text{O}_2$  and is about a factor of 100 larger than the solubilities of  $\text{HO}_2$  and HOONO<sub>2</sub> [22], which should be better models for HOONO. Reducing the estimated solubility by a factor of 100 increases the estimated bond dissociation energy by  $11 \text{ kJ mol}^{-1}$ . Including a factor of 10 uncertainty for the solubility in the error estimate, this yields a gas phase bond dissociation enthalpy of  $99 \pm 11 \text{ kJ mol}^{-1}$ . With a reasonable A-factor of  $10^{15} \text{ s}^{-1}$ , this gives a lifetime towards dissociation for HOONO of 230 seconds, but with an uncertainty factor of nearly 100.

The lifetime for transport of a radical to a particle in the atmosphere is of the order of 200 seconds under clean continental conditions [23] and considerably shorter under more polluted conditions. These transport lifetimes are significantly limited by diffusion so lifetimes for collisions with particle surfaces are a factor of two or three smaller than this. However, collisions with particle surfaces do not always result in reaction. The reaction probability,  $\gamma$ , for isomerization can be estimated from equation (III) [24]:

$$\gamma = \frac{4HRT\sqrt{kD_1}}{\bar{c}} \quad (III)$$

where  $H$  is the Henry's law constant,  $k$  is the first order reaction rate for isomerization,  $D_1$  is the liquid phase diffusion coefficient, and  $\bar{c}$  is the average molecular speed. We take  $H$  to be  $5.3 \times 10^3 \text{ M atm}^{-1}$  to be consistent with the estimate of the bond dissociation energy,  $k$  is  $1.3 \text{ s}^{-1}$  at 298 K in solutions with pH 2 to 6 [21], and we assume a typical value of  $1 \times 10^{-5} \text{ cm}^2 \text{ s}^{-1}$  for  $D_1$ . This yields  $\gamma = 0.06$  and a lifetime towards heterogeneous isomerization on the order of 1000 seconds in clean air and much less in more polluted air.

Within the large error of these estimates, the rates of isomerization and dissociation are comparable. However, there are additional factors that will tend to favor isomerization over dissociation. First, the rate of the isomerization reaction increases below pH 2 [21]. Since atmospheric particles can be highly acidic, this will increase the reaction probability. Second, the ac-

tivation energy for isomerization, ( $75 \text{ kJ mol}^{-1}$ , [21]), is less than the bond dissociation energy. Third, since Henry's Law constants increase with decreasing temperature,  $\gamma$  will also increase at low temperature (c.f. equation III). Thus, as temperatures decrease below 298 K, isomerization will be increasingly favoured.

## CONCLUSION

The water dependence of the loss of  $\text{HO}_2$  radicals to the walls of a reactor has an adverse effect on the performance of the radical amplifier. However, the apparent remaining gas phase dependence has a large effect on not only the radical amplifier but possibly on the chemistry of the atmosphere. To fully understand the observations reported here, and their impact on atmospheric chemistry, requires additional kinetic data on the reaction of radicals with  $\text{NO}_x$  species in the presence of water.

This work was supported by the Atmospheric Environment Service of Environment Canada. We thank G. W. Harris and M. C. Arias for helpful discussions.

## BIBLIOGRAPHY

1. Cantrell, C. A.; Stedman, D. H. *Geophys Res Lett* 1982, 9, 846.
2. Hastie, D. R.; Weissenmayer, M.; Burrows, J. P.; Harris, G. W. *Anal Chem* 1991, 63, 2048.
3. Cantrell, C. A.; Shetter, R. E.; Calvert, J. G.; Parrish, D. D.; Fehsenfeld, F. C.; Goldan, P. D.; Kuster, W.; Williams, E. J.; Westberg, H. H.; Allwine, G.; Martin, R. *J Geophys Res* 1993, 98, 18,355.
4. Arias, M. C.; Hastie, D. R. *Atmos Environ* 1996, 30, 2167.
5. Monks, P. S.; Carpenter, L. J.; Penkett, S. A.; Ayers, G. P. *Geophys Res Lett* 1996, 97, 535.
6. Mihelcic, D.; Klemp, D.; Müsgen, P.; Pätz, H. W.; Volz-Thomas, A. *J Atmos Chem* 1993, 16, 313.
7. Hu, J.; Stedman, D. H. *Anal Chem* 1994, 66, 3384.
8. Heitlinger, M.; Volz-Thomas, A.; Mihelcic, D.; Müsgen, P.; Burrows, J. P.; Andres Hernandez, M. D.; Stöbener, D.; Perner, D.; Arnold, T.; Seuwen, R.; Clemitshaw, K. C.; Penkett, S. A.; Laverdet, G.; El-Boudali, K.; Tenton, S.; Hjorth, J.; Poulida, O.; Hastie, D. R.; Arias, M. C.; Borrell, P.; Borrel, P. M. Peroxy radical InterComparison Exercise II: The oxidizing capacity of the troposphere. Venice, Italy Oct. 24, 1996.
9. Schultz, M.; Heitlinger, M.; Mihelcic, D.; Volz-Thomas, A. *J Geophys Res* 1995, 100, 18,811.
10. Mihele, C. M.; Hastie, D. R. *Geophys Res Lett* 1998, 25, 1911.
11. Clemitshaw, K. C.; Carpenter, L. J.; Penkett, S. A.; Jenkin, M. E. *J Geophys Res* 1997, 102, 25,405.
12. Murphy, D. M.; Fahey, D. W. *Anal Chem* 1987, 59, 2753.
13. Howard, C. J. *J Am Chem Soc* 1980, 102, 6937.
14. Poulet, G.; Laverdet, G.; Le Bras, G. *J Chem Phys* 1984, 80, 1922.
15. Cantrell, C. A.; Shetter, R. E.; Lind, J. A.; McDaniel, A. H.; Calvert, J. G. *J Geophys Res* 1993, 98, 2897.
16. Overend, R.; Paraskevopolous, G.; Black, C. *J Chem Phys* 1976, 64, 4149.
17. Kircher, C. C.; Sander, S. P. *J Phys Chem* 1984, 88, 2082.
18. Sander, S. P.; Peterson, M. E. *J Phys Chem* 1984, 88, 1571.
19. Li, R.-R.; Sauer Jr., M. C.; Sheffield, G. *J Phys Chem* 1981, 85, 2833.
20. Bohn, B.; Zetzsch, C. *J Phys Chem A* 1997, 101, 1488-1493.
21. Koppenol, W. H.; Moreno, J. J.; Pryor, W. A.; Ischiropoulos, H.; Beckman, J. S. *Chem Res Toxicol* 1992, 5, 834-842.
22. Regimbal, J.-M.; Mozurkewich, M. *J Phys Chem* 1997, 101, 8822-8829.
23. Eisele, F. L.; Tanner, D. J. *J Geophys Res* 1993, 98, 9001-9010.
24. Danckwerts, P. V. *Trans Faraday Soc* 1951, 47, 1014-1023.
25. Atkinson, R.; Baulch, D. L.; Cox, R. A.; Hampson Jr., R. F.; Kerr, J. A.; Rassi, M. J.; Troe, J. *J Phys Chem Ref Data* 1997, 524-549.